Title	Temperature dependence of terahertz emission by an asymmetric intrinsic Josephson junction device
Author(s)	Kakeya, Itsuhiro; Hirayama, Nobuo; Omukai, Yuta; Suzuki, Minoru
Citation	Journal of Applied Physics (2015), 117(4)
Issue Date	2015-01-30
URL	http://hdl.handle.net/2433/216403
Right	© 2015 AIP Publishing LLC. This article may be downloaded for personal use only. Any other use requires prior permission of the author and AIP Publishing. The following article may be found at http://scitation.aip.org/content/aip/journal/jap/117/4/10.1063/1.4906849; The full-text file will be made open to the public on 30 January 2016 in accordance with publisher's 'Terms and Conditions for Self-Archiving'.
Type	Journal Article
Textversion	publisher

Temperature dependence of terahertz emission by an asymmetric intrinsic Josephson junction device

Itsuhiro Kakeya, Nobuo Hirayama, Yuta Omukai, and Minoru Suzuki

Citation: Journal of Applied Physics **117**, 043914 (2015); doi: 10.1063/1.4906849
View online: http://dx.doi.org/10.1063/1.4906849
View Table of Contents: http://scitation.aip.org/content/aip/journal/jap/117/4?ver=pdfcov
Published by the AIP Publishing

Temperature dependence of terahertz emission by an asymmetric intrinsic Josephson junction device

Itsuhiro Kakeya,[a] Nobuo Hirayama, Yuta Omukai, and Minoru Suzuki
Department of Electronic Science and Engineering, Kyoto University, Nishikyo-ku, Kyoto 615-8510, Japan

(Received 5 November 2014; accepted 16 January 2015; published online 30 January 2015)

This study investigates the effect of temperature on the emission frequency of an intrinsic Josephson junction terahertz (THz) electromagnetic wave source, which can be used for high-speed communications by THz carrier wave. The characteristic emission features of two device types (asymmetric and symmetric) and two bias regimes (low and high) were determined. The bias-dependent emission frequency was temperature dependent in the asymmetric device, most likely reflecting the temperature-dependent London penetration depth. The bias tunability of the emission frequency can be explained by device self-heating, which significantly and inhomogeneously raises the temperatures of the device from its bath temperature. These findings are consistent with previous studies of temperature distribution in these devices. © *2015 AIP Publishing LLC*.
[http://dx.doi.org/10.1063/1.4906849]

I. INTRODUCTION

Stacks of intrinsic Josephson junctions (IJJs) constructed from the high-T_c superconductor $Bi_2Sr_2CaCu_2O_{8+\delta}$ (Bi2212) emit at terahertz (THz) frequencies. Such IJJ emission has rapidly attracted theoretical and experimental interest.[1–8] The emitted terahertz waves are considered to be monochromatic and coherent because it is attributed to synchronization of stacked Josephson junctions naturally formed inside Bi2212 single crystals. Thus, these IJJs can be used for generating THz waves to realize ultrafast and huge-capacity wireless data transfers. The emission frequencies of these structures (ranging from 0.3 to 0.9 THz) are roughly determined by the geometry of the stacks. Reportedly, the emission power of a single stack of coherently oscillating IJJs and synchronized three stacks can reach 30 μW (Refs. 9 and 10) and 0.6 mW,[11] respectively. The underlying physics behind these phenomena is synchronization of hundreds of IJJs consisting of a stack and synchronization of stacks connected by a base crystal.

To understand the synchronization mechanism, we must elucidate the temperature distribution in the stack. Since the self-generated heat in the voltage state is retained by the low thermal conductivity of the superconducting crystal, localized temperature rise in the stack is inevitable.[12] Local temperature rise above the critical temperature T_c (hotspots) of the emitting devices has been first identified by low-temperature scanning laser microscopy (LTSLM).[5] Although the LTSLM signals reflect changes in the various physical parameters of the stacks, these results predict that coherent oscillation along the *c*-axis arises from spatial inhomogeneity of the junction along the *ab*-plane. Meanwhile, we previously altered the thickness of the electrodes atop the stacks, and found that emission is largely governed by thermal inhomogeneity of the emitting stack itself, which is caused by the weak heat link between the stack and thermal bath.[13] More recently, we have reported that the hotspots are detrimental for emission intensities.[14]

The emission frequency f_e is tuned by changing either the bias current or bath temperature T_b. Benseman *et al.* investigated the temperature dependence of the emission frequency in asymmetric device configuration, namely, a superconducting substrate overlain with a trapezoidal stack. They attributed the frequency-temperature relation to the temperature dependence of the London penetration depth along the *ab*-plane.[15] At a certain temperature, an IJJ included in the stack might entrain IJJs of different resonance frequencies (widths) due to the trapezoidal stack shape, establishing a tuning bandwidth.[16] The amplitude of the Josephson oscillation has a node at the superconducting substrate because the substrate and stacked IJJs are in the superconducting (zero-voltage) and voltage state, respectively.

Two emission regimes have been recognized: a low-bias regime well below the critical current in the voltage state, and a high-bias regime, in which the current exceeds the critical current. The high-bias regime admits a rich variety of phenomena, such as wide-range frequency tuning, hotspot formation, and a sharp spectrum linewidth, whereas less complicated behavior is observed in the low-bias regime.[17–19] Although the high-bias emission presumably linked to temperature inhomogeneity, no systematic difference between the frequency tuning of high-bias and low-bias emissions has been reported to date.

In this letter, we discuss how the emission frequency f_e is affected by temperature in three devices. Low-bias emission from the mesa device is explained by the T_b dependence of the London penetration depth, whereas the high-bias emission is attributed to significant temperature rise from T_b and temperature inhomogeneity in the device. Different from the asymmetric mesa device, low-bias emission from the symmetric stand-alone stack is independent of T_b because no nodal Josephson oscillation is established along the *c*-axis.

II. EXPERIMENTS

We prepared three devices from $Bi_2Sr_2CaCu_2O_{8+\delta}$ single crystals grown by the traveling solvent floating zone method. Device A and C are ordinary mesa devices comprising IJJ stacks formed on bulk single crystals by

[a]kakeya@kuee.kyoto-u.ac.jp

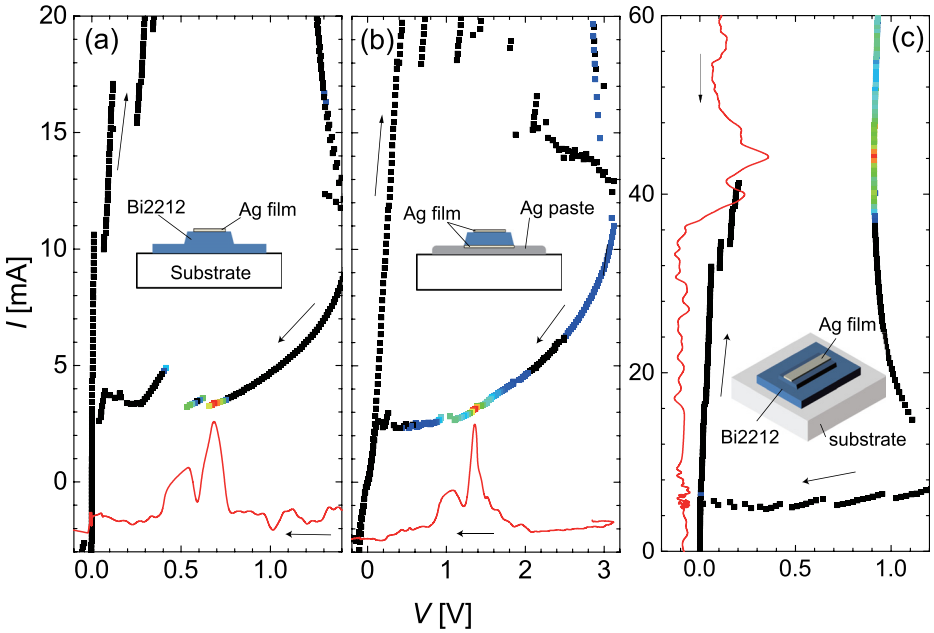

FIG. 1. IV characteristics (symbols) and bolometer responses (solid lines) in device A (a), B (b), and C (c) at 25 K. Solid red curves are the bolometer outputs as functions of V for (a) and (b) and as a function of I for (c). The amplitudes of the bolometer output correspond to plot the colors of the I–V plots. Arrows represent scan directions. Device configurations are depicted in the insets.

photolithography and the Ar milling technique as described in the previous works. Device B is a stand-alone stack.[18] An IJJ stack was removed from a bulk crystal and glued onto a sapphire substrate with silver epoxy. The stack was sandwiched between a pair of silver electrodes formed by a vacuum evaporation technique. Schematics of the three devices are depicted in the insets of Fig. 1. The stacks were approximately 400 μm long, but their widths w and thicknesses t ranged from 60 to 90 μm and 1.1 to 1.8 μm, respectively. The geometries of the devices are summarized in Table I.

To precisely determine the temperature dependence of f_e, we measured emission spectra of the devices by a laboratory-designed high-resolution FT-IR spectrometer[20] after checking THz wave emission using a simple detection system.[13] The frequency resolution of the spectrometer is less than 1 GHz, an order of magnitude higher than that of an ordinary commercial FT-IR spectrometer, enabling precise determination of the temperature effect on f_e. The bath temperature T_b was measured at the copper sample stage, to which the device was glued with silver paste. The devices on their copper stages were placed in a vacuum and the emitted THz waves passed through a white polyethylene window.

III. RESULTS AND DISCUSSION

A. Device A: Low bias regime

THz frequencies were emitted from Device A within a limited bias region in the low-bias regime, as shown in Fig. 1(a). The emission was observed between 15 and 45 K just above the discontinuity in the I–V characteristics (retrap). The emission range is $0.5 < V < 0.8$ V and $3 < I < 4$ mA, and the detected intensity roughly decreases with increasing T_b. The emission spectra at various T_bs are shown in Fig. 2(a). At 25 K, the peak frequency and spectrum width are 450 and 2.2 GHz, respectively. Through the AC Josephson relation $2ev = \hbar\omega$, the frequency $\omega/2\pi$ corresponds to a junction voltage $v = 0.92$ mV/IJJ. Thus, the total voltage across the device is $Nv = 0.74$ V, where N is the number of IJJs ($N \simeq 800$), which approximately matches the bias voltage at the peak intensity $V_e = 0.76$ V. As T_b increases, f_e decreases, maintaining the AC Josephson relation within a few percent. The spectrum width is independent of T_b and is narrower than that obtained by heterodyne

TABLE I. List of samples used in this study. w_t and w_b represent the top and bottom widths of the stack, respectively. For the analysis, the averaged width $w = (w_t + w_b)/2$ is used in the text. The stack thickness t and the critical temperature T_c of the device are shown.

	Type	w_t (μm)	w_b (μm)	t (μm)	T_c (K)
A	Mesa	82.1	92.3	1.19	72
B	Stand-alone	64.5	75.5	1.80	70
C	Mesa	65.5	74.3	1.11	91.5

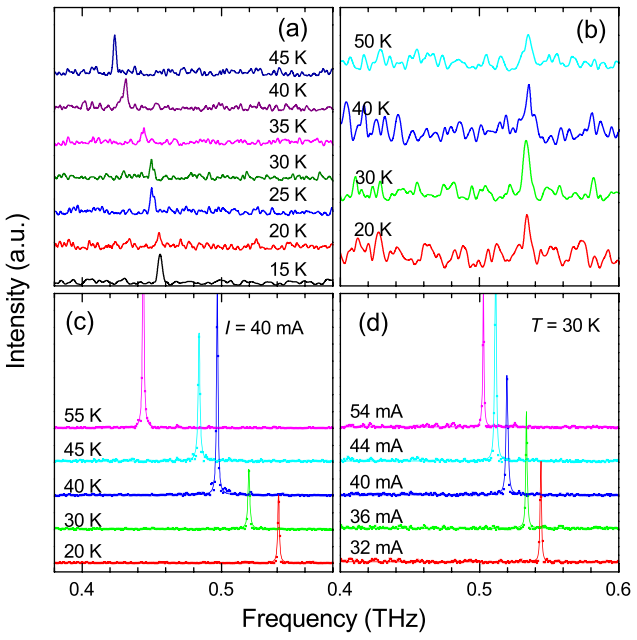

FIG. 2. Emission spectra at various T_bs in device A (a), B (b), and C (c). Panel (d) shows the bias dependence of the spectra in device C.

mixing, in which poor coherence of the low-bias emission has been claimed.[19]

The temperature dependence of f_e is plotted in Fig. 3(a). Temperature-frequency relations of the standing waves in a resonator are given by temperature dependence of the propagation velocity of electromagnetic waves inside the resonator (the so-called Swihart velocity for a single Josephson junction). Josephson plasma waves with both k_x (parallel to the *ab*-plane) and k_z (parallel to the *c*-axis) may be excited in an IJJ stack; thus, the propagation velocity is estimated as $\tilde{c}^2 = c_0^2[\epsilon_c 2\{1-\cos(k_z s)\}\lambda_{ab}/s^2+1]^{-1}$, where k_z, λ_{ab}, and s are the wavenumber of the standing wave along the *c*-axis, the London penetration depth along the *ab*-plane, and the thickness of the superconducting layers, respectively.[21] Benseman *et al*. suggested that if the boundary conditions of the stack are asymmetric with respect to the *c*-axis, an asymmetric standing wave is established along the *c*-axis with $k_z = m\pi/2t$ ($m = 1, 3, \ldots$), where t is the thickness of the stack.

Since the length of the stack is sufficiently longer than the width, standing wave with k_x along the width is dominant. Furthermore, $2\pi/k_z = 2t \sim 10^3$ s and $f_e \gg \omega_p/2\pi$ hold. Finally, the frequency of the two-dimensional standing wave is given by

$$f = \frac{c_0}{2w\sqrt{\epsilon_c\{1+(m\pi\lambda_{ab}(T)/2t)^2\}}}. \quad (1)$$

The frequency f depends on temperature because $\lambda_{ab}(T)$ is a temperature-dependent parameter, as measured by several authors.[22–24] The solid curve in Fig. 3(a) plots Eq. (1) as a function of temperature, using the data of Anukool *et al*. data with the amount of doping $p = 0.124$ (determined by the T_c of the Device A).[22] Setting the refractive index $n = \sqrt{\epsilon_c} = 3.35$, $m = 1$, and $w = 87\,\mu$m, an excellent agreement is obtained between Eq. (1) and the experimental data.

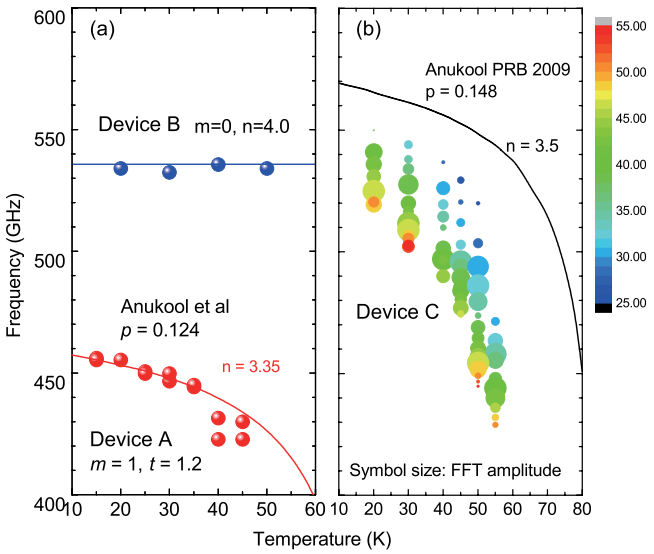

FIG. 3. Temperature dependence of the emission frequency from devices (a) A, B, and (b) C. Solid lines are values of Eq. (1) with parameters given in the figures. Data of $\lambda_{ab}(T)$ are obtained from Ref. 22 with close T_c. Symbol color in (b) represents bias current according to the color bar at right and symbol size means FFT amplitude of the spectra.

B. Device B: Stand-alone IJJ stack

The *I*–*V* characteristics and emission intensities of Device B are plotted in Fig. 1(b). The intensity sharply peaks at 1.38 V and a weaker peak appears at 1.10 V. Device B emitted THz radiation in the low-bias regime. Figure 2(b) shows the FT-IR spectra taken at optimum bias points at various temperatures. Note that f_e ($\simeq$540 GHz) is independent of temperature between 10 and 50 K in a sharp contrast to mesa-type devices, whose emission frequencies decrease with increasing T_b.

We interpret the insensitivity of f_e to the temperature in Device B as follows. The highly conducting silver electrodes are affixed to the top and bottom of the stand-alone stack; moreover the whole stack possibly becomes uniformly resistive because of the absence of superconducting substrate. The symmetric stack configuration admits excitation of the $m = 0$ uniform mode rendering Eq. (1) independent of $\lambda_{ab}(T)$. Through the AC Josephson relation, $f \simeq 540$ GHz corresponds to 1.11 mV per IJJ, resulting in 1.35 V across the whole stack of $N = 1200$. This voltage is quite close to prominent peak bias voltage (1.38 V), supporting that $m = 0$ standing waves are excited along the *c*-axis.

The refractive index $n = c_0/2wf_e$ was considerably higher in Device B than in the other two devices, presumably because the effective width of the stack was considerably shorter than w in this device. The edges and surfaces of stand-alone stack are more deteriorated by organic solvents and water than those of typical mesa devices, because of the complicated fabrication process and the large surface area. Similar results for stand-alone stacks and focused-ion-beam-milled mesas have been reported in previous studies.[18,25]

C. Device C: High-bias regime

Device C demonstrates high-bias emission. The high-bias regime covers the region $30 < I < 60$ mA and $0.7 < V < 0.9$ V, as shown in Fig. 1(c). Figures 2(c) and 2(d) present the spectra of the high-bias emissions at various temperatures with a constant bias current of 40 mA, and at various bias currents with $T_b = 30$ K, respectively. As the temperature increases from 20 to 60 K, f_e decreases from 0.54 to 0.43 THz. Increasing the bias current similarly decreases the f_e. From this result, we attribute the decrease in f_e to the increase in effective temperature of the stack as $\tilde{c}$ decreases. The emission frequencies at different T_b and bias conditions are plotted in Fig. 3(b). Obviously, f_e decreases as either T_b or bias increases; however, these experimental results are considerably lower than the predictions of Eq. (1) with $\lambda_{ab}(T)$ determined by its p as well as in Device A. The theoretical curve may overlap with the experimental data shifted toward higher temperatures along the temperature axis. It is interpreted that in the high-bias regime, the effective temperature giving rise to $\tilde{c}$ is significantly higher than T_b, in sharp contrast to the results of Device A.

These results suggest a highly inhomogeneous temperature distribution in the high-bias regime. This is consistent with previous imaging measurements[5,11,14] and numerical calculations.[12,26] Figure 4(a) plots f_e (solid symbols) as a function of the *c*-axis biased resistance $\bar{R}_c = V/I$, corrected

by subtracting the contact resistance (included in Fig. 1(c)). Assuming that the $\bar{R}_c$ corresponds to the quasiparticle resistance at the effective stack temperature $T > T_b$, a homogeneous temperature distribution would yield single values of Eq. (1) and $\bar{R}_c(T)$; accordingly, these plots should collapse onto a single line. Instead, the R_c reduces as T_b is lowered. This deviation can be explained by considering an inhomogeneous temperature distribution and a temperature dependence of both $f(T)$ and $\tilde{c}(T)$ as described in the following paragraph.

As a toy model of an IJJ stack with strong temperature inhomogeneity, we consider two linked IJJ stacks 1 and 2 with the equal volume and uniform temperature T_1 and T_2 electrically connected in parallel as shown in Fig. 4(b). This models a device with a hotspot (lower resistance) region shunting a lower temperature (higher resistance) region. The excited electromagnetic wave propagates inside the media with refractive indices n_1 and n_2 connected in series without reflection at their interface. T_1 (T_2) is δT higher (lower) than the average temperature T_0, i.e., $T_1 = T_0 + \delta T$, $T_2 = T_0 - \delta T$. The measured resistance $\bar{R}_c(T_b)$ is considered as the parallel connection of $R_c(T_1) = R_c(T_0) - \delta R_c$ and $R_c(T_2) = R_c(T_0) + \delta R_c$, where $R_c(T)$ represents the intrinsic c-axis resistance of the stack at temperature T. Consequently, we obtain $\bar{R}_c(T_b) = R_c(T_0)[1 - (\delta R_c/R_c(T_0))^2]$, which shows that decrease in $\bar{R}_c(T_b)$ from $R_c(T_0)$ is more significant for larger δT. This situation is more pronounced at lower temperature because the thermal conductivity is smaller. On the other hand, the measured emission frequency f_e is determined by the distribution in the effective refractive index given by $\tilde{n}(T) = \sqrt{\epsilon_c\{1 + (\pi\lambda_{ab}(T)/2t)^2\}}$. Assuming $\tilde{n}(T_1) = \tilde{n}(T_0) + \delta\tilde{n}$ and $\tilde{n}(T_2) = \tilde{n}(T_0) - \delta\tilde{n}$, measured refractive index $\bar{n}(T_b) = \{\tilde{n}(T_1) + \tilde{n}(T_2)\}/2$. Therefore, we can simply state $\bar{n}(T_b) = \tilde{n}(T_0)$, which corresponds to $f_e(T_b) = f(T_0)$ given by Eq. (1); that is, the measured emission frequency f_e is directly determined by the average temperature T_0. From this simplified consideration and comparison with the homogeneous case, we infer that temperature inhomogeneity is responsible for decreases in $\bar{R}_c(T_b)$ with respect to $f_e(T_b)$. Since the temperature distribution in Bi2212 IJJ stacks emitting at terahertz frequencies becomes more homogeneous at higher temperatures,[27] the quantity $\bar{R}_c(T_b) - R_c(T_0)$ due to the temperature inhomogeneity becomes more remarkable at lower T_b, where δR_c is larger even for a certain δT. This conclusion is consistent with the plots in Fig. 4(a), which shift toward lower $\bar{R}_c$ (left) as δR_c increases at lower T_b. A comparison between $\bar{R}_c$ and $R_c - T$ data allows to estimate an average temperature T_0 of the stack. As a result, T_0s are roughly estimated as 100 and 60 K for $\bar{R}_c = 15$ and 30 Ω, respectively. The mean-field critical temperature of the device being 91.5 K also supports the strong temperature inhomogeneity of the device.

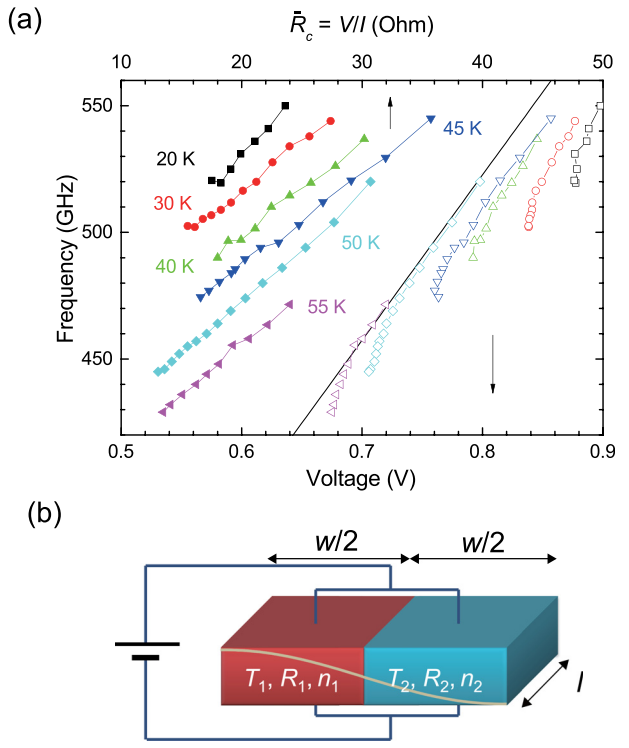

FIG. 4. (a) Plots of emission frequency f_e vs averaged resistance $\bar{R}_c$ (filled symbols; top axis) and bias voltage V (open symbols; bottom axis) of Device C. The same colors represent data at the same temperature. The solid line is the ac Josephson relation. (b) Toy model of a mesa with an inhomogeneous temperature distribution. A gray solid curve represents the excited electromagnetic wave inside the stack.

The present interpretation does not include the stacking effect of IJJs. Benseman *et al.*,[28] have discussed the excess c-axis voltage with respect to the emission frequency due to temperature inhomogeneity along the c-axis. Synchronized IJJs closer to the mesa surface (electrode) arise equal voltage per IJJ, while unsynchronized IJJs closer to the substrate (thermal bath) arise higher voltage per IJJ because of the negative temperature dependence of the quasiparticle resistance. The excess voltage due to the unsynchronized IJJs is higher at lower T_b. Their argument is also valid for the present result, where the bias voltage is higher than the value estimated from the emission frequency via the ac Josephson relation as plotted as open symbols in Fig. 4(a). Since the behavior of $f_e - \bar{R}_c$ plots looks irrelevant to the deviation from the ac Josephson relation (solid line), we consider that the present results indicate both in-plane and out-of-plane strong temperature inhomogeneities.

IV. SUMMARY

This study demonstrated the qualitative difference in the temperature dependence of the frequencies emitted by usual mesa IJJ stacks and a stand-alone IJJ stack. These trends were predicted in previous work by Benseman *et al.*[15] By considering a toy model, we attributed the significant bias tuning at a fixed bath temperature to inhomogeneous temperature rise of the stack (relative to the bath temperature). The linewidths of the emission spectra were less than 1 GHz, regardless of emission type. These results strongly contrast with those of Li *et al.*,[19] who reported poor synchronization of stacked IJJs in the low-bias region.

ACKNOWLEDGMENTS

The authors acknowledge M. Tsujimoto, A. Elarabi, Y. Maeda, Y. Kamei, T. Nakagawa, Y. Nakagawa, S. Mizuta, T. Yamamoto, and K. Kadowaki for their technical

assistance. Comments from A. Koshelev, T. Koyama, and X. Hu are greatly appreciated. This work was supported by KAKENHI (23681030).

[1]L. Ozyuzer, A. E. Koshelev, C. Kurter, N. Gopalsami, Q. Li, M. Tachiki, K. Kadowaki, T. Yamamoto, H. Minami, H. Yamaguchi, T. Tachiki, K. E. Gray, W. K. Kwok, and U. Welp, Science **318**, 1291 (2007).
[2]K. Kadowaki, H. Yamaguchi, K. Kawamata, T. Yamamoto, H. Minami, I. Kakeya, U. Welp, L. Ozyuzer, A. E. Koshelev *et al.*, Phys. C **468**, 634 (2008).
[3]S. Lin and X. Hu, Phys. Rev. Lett. **100**, 247006 (2008).
[4]H. Minami, I. Kakeya, H. Yamaguchi, T. Yamamoto, and K. Kadowaki, Appl. Phys. Lett. **95**, 232511 (2009).
[5]H. B. Wang, S. Guénon, J. Yuan, A. Iishi, S. Arisawa, T. Hatano, T. Yamashita, D. Koelle, R. Kleiner, and S. Guenon, Phys. Rev. Lett. **102**, 017006 (2009), e-print arXiv:0807.2749.
[6]T. Koyama, H. Matsumoto, M. Machida, and K. Kadowaki, Phys. Rev. B **79**, 104522 (2009).
[7]X. Hu and S.-Z. Lin, Supercond. Sci. Technol. **23**, 053001 (2010).
[8]U. Welp, K. Kadowaki, and R. Kleiner, Nat. Photonics **7**, 702 (2013).
[9]K. Yamaki, M. Tsujimoto, T. Yamamoto, A. Furukawa, T. Kashiwagi, H. Minami, and K. Kadowaki, Opt. Express **19**, 3193 (2011), e-print arXiv:1005.2341v1.
[10]S. Sekimoto, C. Watanabe, H. Minami, T. Yamamoto, T. Kashiwagi, R. A. Klemm, and K. Kadowaki, Appl. Phys. Lett. **103**, 182601 (2013).
[11]T. M. Benseman, K. E. Gray, A. E. Koshelev, W.-K. Kwok, U. Welp, H. Minami, K. Kadowaki, and T. Yamamoto, Appl. Phys. Lett. **103**, 022602 (2013).
[12]A. Yurgens, Phys. Rev. B **83**, 184501 (2011).
[13]I. Kakeya, Y. Omukai, T. Yamamoto, K. Kadowaki, and M. Suzuki, Appl. Phys. Lett. **100**, 242603 (2012).
[14]M. Tsujimoto, H. Kambara, Y. Maeda, Y. Yoshioka, Y. Nakagawa, and I. Kakeya, Phys. Rev. Appl. **2**, 044016 (2014).
[15]T. M. Benseman, A. E. Koshelev, K. E. Gray, W.-K. Kwok, U. Welp, K. Kadowaki, M. Tachiki, and T. Yamamoto, Phys. Rev. B **84**, 064523 (2011).
[16]K. Wiesenfeld, P. Colet, and S. Strogatz, Phys. Rev. Lett. **76**, 404 (1996).
[17]H. Wang, S. Guénon, B. Gross, J. Yuan, Z. Jiang, Y. Zhong, M. Grünzweig, A. Iishi, P. Wu, T. Hatano, D. Koelle, and R. Kleiner, Phys. Rev. Lett. **105**, 057002 (2010).
[18]M. Tsujimoto, T. Yamamoto, K. Delfanazari, R. Nakayama, T. Kitamura, M. Sawamura, T. Kashiwagi, H. Minami, M. Tachiki, K. Kadowaki, and R. A. Klemm, Phys. Rev. Lett. **108**, 107006 (2012).
[19]M. Li, J. Yuan, N. Kinev, J. Li, B. Gross, S. Guénon, A. Ishii, K. Hirata, T. Hatano, D. Koelle, R. Kleiner, V. Koshelets, H. Wang, and P. Wu, Phys. Rev. B **86**, 060505 (2012).
[20]I. Kakeya, N. Hirayama, T. Nakagawa, Y. Omukai, and M. Suzuki, Phys. C **491**, 11 (2013).
[21]R. Kleiner, Phys. Rev. B **50**, 6919 (1994).
[22]W. Anukool, S. Barakat, C. Panagopoulos, and J. R. Cooper, Phys. Rev. B **80**, 024516 (2009).
[23]T. Jacobs, S. Sridhar, Q. Li, G. Gu, and N. Koshizuka, Phys. Rev. Lett. **75**, 4516 (1995).
[24]S.-F. Lee, D. Morgan, R. Ormeno, D. Broun, R. Doyle, J. Waldram, and K. Kadowaki, Phys. Rev. Lett. **77**, 735 (1996).
[25]T. Kashiwagi, K. Yamaki, M. Tsujimoto, K. Deguchi, N. Orita, T. Koike, R. Nakayama, H. Minami, T. Yamamoto, R. A. Klemm, M. Tachiki, and K. Kadowaki, J. Phys. Soc. Jpn. **80**, 094709 (2011).
[26]B. Gross, J. Yuan, D. Y. An, M. Y. Li, N. Kinev, X. J. Zhou, M. Ji, Y. Huang, T. Hatano, R. G. Mints, V. P. Koshelets, P. H. Wu, H. B. Wang, D. Koelle, and R. Kleiner, Phys. Rev. B **88**, 014524 (2013).
[27]H. Minami, C. Watanabe, K. Sato, S. Sekimoto, T. Yamamoto, T. Kashiwagi, R. A. Klemm, and K. Kadowaki, Phys. Rev. B **89**, 054503 (2014).
[28]T. M. Benseman, A. E. Koshelev, W.-K. Kwok, U. Welp, K. Kadowaki, J. R. Cooper, and G. Balakrishnan, Supercond. Sci. Technol. **26**, 085016 (2013).